



UNIVERSITY OF LEEDS

This is a repository copy of *The effect of interactions between rainfall patterns and land-cover change on flood peaks in upland peatlands*.

White Rose Research Online URL for this paper:  
<http://eprints.whiterose.ac.uk/138096/>

Version: Accepted Version

---

**Article:**

Gao, J, Kirkby, M and Holden, J [orcid.org/0000-0002-1108-4831](https://orcid.org/0000-0002-1108-4831) (2018) The effect of interactions between rainfall patterns and land-cover change on flood peaks in upland peatlands. *Journal of Hydrology*, 567. pp. 549-559. ISSN 0022-1694

<https://doi.org/10.1016/j.jhydrol.2018.10.039>

---

© 2018 Elsevier B.V. Licensed under the Creative Commons Attribution-Non Commercial No Derivatives 4.0 International License (<https://creativecommons.org/licenses/by-nc-nd/4.0/>).

**Reuse**

This article is distributed under the terms of the Creative Commons Attribution-NonCommercial-NoDerivs (CC BY-NC-ND) licence. This licence only allows you to download this work and share it with others as long as you credit the authors, but you can't change the article in any way or use it commercially. More information and the full terms of the licence here: <https://creativecommons.org/licenses/>

**Takedown**

If you consider content in White Rose Research Online to be in breach of UK law, please notify us by emailing [eprints@whiterose.ac.uk](mailto:eprints@whiterose.ac.uk) including the URL of the record and the reason for the withdrawal request.



[eprints@whiterose.ac.uk](mailto:eprints@whiterose.ac.uk)  
<https://eprints.whiterose.ac.uk/>

1 **The effect of interactions between rainfall patterns and**  
2 **land-cover change on flood peaks in upland peatlands**

3 Jihui Gao<sup>1, 2, 3\*</sup>, Mike Kirkby<sup>2</sup>, Joseph Holden<sup>2</sup>

4 1. State Key Laboratory of Hydraulics and Mountain River Engineering,  
5 Sichuan University, Chengdu, 610065, China

6 2. water@leeds, School of Geography, University of Leeds, Leeds, LS2 9JT,  
7 UK

8 3. School of Water Resource & Hydropower, Sichuan University, Chengdu  
9 610065, China

10 ***Abstract***

11 Flood processes in catchments are driven by a combination of rainfall and  
12 landscape characteristics. Upland peatlands are source areas of flooding but  
13 there is lack of understanding of how different rainfall intensities and  
14 temporal patterns may interact with land-cover configurations to influence  
15 flood peaks. Using spatially distributed (SD-) TOPMODEL we investigated  
16 these interactions for a case study peatland catchment. For each of four  
17 rainfall depths ranging from 20 mm to 50 mm, four storm rainfall patterns  
18 were applied (rainfall that was uniform, rainfall with an early peak intensity  
19 during the storm, middle peak and late peak). Late peak rainfall resulted in  
20 the highest river flow peaks at the catchment outlet studied, followed by  
21 middle and early rainfall peak patterns, while uniform rainfall through time  
22 gave the lowest flow peaks. A key factor was synchronicity of overland flow  
23 movement and concentration. The impact on river flow peaks of land-cover  
24 change on riparian zones and on gentle gradient slopes was larger than that  
25 for other parts of the catchment under different rainfall intensities and  
26 patterns. The impacts of land-cover change on proportional change in flood  
27 peaks in these sensitive areas became smaller when rainfall intensity  
28 increased, but absolute changes in flow peaks became larger. Land-cover  
29 change in sensitive areas under middle and late peak rainfall had a larger  
30 impact on river flow peaks than for early peak rainfall. It was possible to  
31 identify the 'worst' rainfall patterns for a particular case of land-cover change  
32 which may be useful for practitioners to help manage expectations of flood  
33 response to nature-based solutions.

34 **Keywords:** rainfall characteristics, land management, peak flow, overland  
35 flow, nature-based solutions, TOPMODEL.

## 36 ***1 Introduction***

37 Runoff processes in natural catchments are driven by a combination of  
38 rainfall patterns and landscape characteristics. Every rainfall event has a  
39 unique temporal rainfall distribution, but sometimes patterns of this  
40 distribution in a particular catchment can be generalized from historic rainfall  
41 data (e.g. Dolsak et al., 2016; Huff, 1967; Willems, 2000). Changes in  
42 temporal rainfall distributions in a region are due to both climatic change and  
43 climatic variability (Yilmaz et al., 2014). Temporal rainfall distributions can  
44 impact overland flow and flood processes. Generally, with the same total  
45 amount of rainfall, non-uniform temporal patterns are considered to produce  
46 higher flow peaks than those with uniform patterns. A storm with rainfall of  
47 higher intensity near the end of the storm (late rainfall peak) rather than at  
48 the start or middle of the storm is believed to generate a higher flow peak  
49 than a storm with the same total rainfall but which has greatest rainfall  
50 intensity near the start of the event (Dunkerley, 2012; Dunkerley, 2014).  
51 Some studies have shown that this could be related to soil surface sealing  
52 arising in response to the higher intensity part of the storm (Flanagan et al.  
53 (1988). Other research has attributed the effect to reductions in soil  
54 infiltration capacity during late rainfall compared with earlier in the rainfall  
55 event (Dunkerley, 2012; Xue and Gavin, 2007).

56 Peatlands cover around 423 million ha (Xu et al., 2018) and store more than  
57 half of the world's soil carbon (Yu et al., 2010). Peatlands often occur in  
58 upland areas in temperate and boreal zones where there is a high rainfall  
59 excess (Gallego-Sala and Prentice, 2013). Blanket peat exists on open and  
60 rolling landscapes, typically in oceanic regions which are wet and cool in  
61 climate (Evans and Warburton, 2007). Vascular plants and bryophytes such  
62 as *Sphagnum* are usually form dominant vegetation cover in blanket  
63 peatlands (Holden et al., 2015). Around 15 % of the UK is covered by  
64 blanket peat, where it is mainly found in upland headwater catchments.

65 Upland blanket peatlands, normally with shallow water tables, produce  
66 minimal baseflow but are quickly saturated during rainfall events (Evans et  
67 al., 1999; Price, 1992). Typically, upland blanket peatlands in the UK are  
68 subject to light frontal rainfall (<10 mm hr<sup>-1</sup>) but very occasionally storm  
69 intensities of 20-50 mm hr<sup>-1</sup> can occur which may lead to downstream  
70 flooding. Saturation-excess overland flow dominates the hillslope

71 contributions to the river channel hydrograph in upland blanket peat, even  
72 during light rainfall events (Holden and Burt, 2002; Holden and Burt, 2003).  
73 Hence, upland peatlands are flashy hydrological systems and sensitive to  
74 precipitation characteristics and land-cover modifications. For such systems,  
75 reductions of soil infiltration capacity during storms and sealing of the  
76 surface due to rain drops may be of minimal importance in determining the  
77 river flow peak response to rainfall. Rather, the prime impacts of rainfall  
78 pattern on flow peaks in blanket peatlands could be related to overland flow  
79 delivery and concentration on hillslopes. However, this has never been  
80 tested. Different temporal profiles of precipitation could generate varying  
81 overland flow depths and velocities for every point on hillslopes, which  
82 results in different spatial distributions of overland flow in the catchment for  
83 every time point in a flood event. Thus the synchronicity of overland flow  
84 concentration driven by temporal rainfall patterns could be a key determinant  
85 for river flood formation from peat catchments (Gao et al., 2016). Changes in  
86 such overland flow velocities and patterns may produce different river flow  
87 peak timings and magnitudes.

88

89 In recent years, 'natural flood management' also known as 'nature-based  
90 solutions' has been advocated as a sustainable measure to reduce flood risk  
91 and as a complementary measure to traditional flood management (SEPA,  
92 2011). Natural flood management deals with the sources and pathways of  
93 floodwaters and manipulates river flow at the catchment scale (Holstead et  
94 al., 2017; SEPA, 2011). It includes altering, restoring or using landscape  
95 features to manage flood risk, with practices such as exclusion of grazing  
96 animals, vegetation restoration, creating porous surfaces, or use of small  
97 storage ponds and scrapes to create landscape roughness and water  
98 storage. However, there is a paucity of evidence for evaluating such nature-  
99 based solutions for their flood-attenuation performance under a range of  
100 rainfall patterns (Dadson et al., 2017; Rogger et al., 2017). For upland  
101 blanket peatlands, as overland flow is common, even when peat has been  
102 disturbed by drainage (Holden et al., 2006), then potentially one of the most  
103 effective ways of delaying streamflow using natural flood management is to  
104 create a rough, well-vegetated surface (Ballard et al., 2011; Gao et al., 2016;  
105 Gao et al., 2017; Lane and Milledge, 2013). Such rough revegetation most  
106 commonly occurs for disturbed peatlands where mosses are encouraged to  
107 re-establish in bare areas or to act as an understory to existing sedge and  
108 shrub cover (Parry et al., 2014). The additional motivation for managers is

109 that re-establishment of mosses on peatlands is seen to provide other  
110 functional benefits including enhanced carbon capture and attenuation of  
111 methane release (Larmola et al., 2010).

112

113 The modelling studies by Gao et al. (2016) and Gao et al. (2017) indicated  
114 that the same land-cover change in 'sensitive' areas of upland peat  
115 catchments (e.g. riparian zones and gentle slope areas) could have three  
116 times the impact on river flow peaks as those same land-cover changes in  
117 'insensitive' areas such as headwater regions and steep slopes. However,  
118 these modelling studies used only simple designs of moderate rainfall events  
119 (i.e. 1-hour rainfall pulses with uniform rates of 15 mm hr<sup>-1</sup>, 20 mm hr<sup>-1</sup>, and  
120 30 mm hr<sup>-1</sup>). Larger intensities of rainfall were not studied. Furthermore,  
121 even if the total rainfall depths of storms are kept identical, varying rainfall  
122 profiles (i.e. different temporal distributions of precipitation) could still change  
123 the spatial distribution of overland flow production and synchronicity of  
124 overland flow concentration on hillslopes resulting in differences in river  
125 hydrographs. Therefore, we do not know whether the sensitive parts of  
126 upland catchments recognized in the study of Gao et al. (2016) are still the  
127 most sensitive for different rainfall intensities and patterns. We also do not  
128 know how land-cover change in these areas affects flood peaks for different  
129 distributions of rainfall events. This interaction information would be  
130 important to support expectations by natural flood management practitioners  
131 on the consistencies or inconsistencies of performance of land-cover change  
132 solutions in upland systems to rainfall events. Accordingly, using numerical  
133 modelling methods, this paper aims to investigate the impacts of rainfall  
134 characteristics on river flow peaks during flood events in an upland blanket  
135 peat catchment, and to study the interactions between rainfall characteristics  
136 and land-cover change.

137

## 138 ***2 Methodology***

### 139 **2.1 Study site**

140 The Trout Beck catchment (54°41' N, 2°23' W) is located in the Moor House  
141 National Nature Reserve and covers an area of 11.4 km<sup>2</sup> with an elevation  
142 ranging from 842 m to 533 m in the North Pennine region of northern  
143 England (see Figure 1). It is a headwater tributary of the River Tees, and  
144 90% of the area is covered by blanket peat with a typical depth of 1-2 m

145 (Evans et al., 1999). Large areas of the catchment have re-vegetated with  
146 *Sphagnum* and *Eriophorum* in recent decades after the peat suffered  
147 widespread erosion in the 1950s-1970s (Grayson et al., 2010). The  
148 catchment is mainly covered by a *Calluna-Eriophorum* vegetation  
149 association with a slowly increasing *Sphagnum* abundance in the  
150 understory. Over 630 m, *Calluna is absent and Eriophorum is dominant*  
151 (Evans et al., 1999). The climate of the catchment is sub-arctic oceanic  
152 (Manley, 1942) and there is a mean annual rainfall of 2012 mm based on  
153 rainfall records from 1951 to 1980 and 1991 to 2006 (Holden and Rose,  
154 2011).

155

## 156 **2.2 SD-TOPMODEL**

157 The original TOPMODEL was a lumped or semi-distributed model of  
158 catchment hydrology when developed by Beven and Kirkby (1979). Gao et  
159 al. (2015) developed a spatially-distributed version - SD-TOPMODEL - which  
160 retains the key catchment scale equations of runoff production from the  
161 original TOPMODEL (see Kirkby, 1997) but downscales those equations to  
162 cell scale (using grid cells as computational units). A new overland flow  
163 module was constructed in SD-TOPMODEL by Gao et al. (2015) to  
164 represent overland flow delivery and routing. The overland flow module  
165 employed the multiple-direction flow theory of Quinn et al. (1991) and an  
166 empirically-derived form of the Darcy-Weisbach equation (Holden et al.,  
167 2008). Thus, the SD-TOPMODEL takes topography, surface roughness and  
168 water depth into account to represent overland flow movement in  
169 catchments. In SD-TOPMODEL, there is a dynamic interaction between  
170 overland flow and subsurface flow for each computational cell, and overland  
171 flow from upslope cells can infiltrate into soil in downslope cells in a  
172 catchment. There are major advantages of SD-TOPMODEL for our study.  
173 The model can explicitly simulate the locations of overland flow generation,  
174 the rates of overland flow production, the depths of overland flow, the  
175 pathways of overland flow movement, and the locations of overland flow  
176 infiltrating into soil or entering river channels in any time step during and  
177 after a storm with time-varying precipitation intensities. SD-TOPMODEL also  
178 represents the variation of overland flow velocity according to the surface  
179 roughness presented by the land cover, taking gradient and flow depth into  
180 account.

181

182 There are three key parameters for peatland catchment modelling in SD-  
183 TOPMODEL as defined by Gao et al. (2015):  $K$  is the hydraulic conductivity  
184 of the soil;  $m$  is a scaling parameter representing the active water storage in  
185 soil; and  $k_v$  is an overland flow velocity parameter related to surface  
186 roughness. The model was calibrated and validated by using the GLUE  
187 (generalized likelihood uncertainty estimation) method (Beven and Binley,  
188 1992) of which details can be found in Gao et al. (2015). Values of  
189  $m=0.0055$  m and near-surface  $K=100$  m hr<sup>-1</sup> had good performance (i.e.  
190 Nash-Sutcliffe efficiency > 0.8 in both the model calibration and validation in  
191 the Trout Beck catchment). This well-performing parameter set was used to  
192 run the model for all scenarios, in order to retain consistency in comparing  
193 the scenarios. The results of scenario modelling could be impacted by the  
194 uncertainty of this single parameter set, but the large consumption of  
195 computational time for the GLUE method was not possible for direct  
196 application in this study. However, uncertainties in the model have  
197 previously been investigated by Gao et al. (2016). In this study using the  
198 GLUE framework, 50 parameter sets, in which each set included three  
199 parameters (i.e.  $m$ ,  $K$ ,  $k_v$ ), were randomly selected for three different study  
200 catchments (including Trout Beck catchment) in its representative parameter  
201 space and used to run the model in the calibration period 50 times. The top  
202 five parameter sets with the highest Nash-Sutcliffe efficiencies (all >0.82)  
203 were obtained for each catchment that they studied (the five sets performed  
204 well also in validation periods). They were then used in land cover scenario  
205 runs (only  $k_v$  was changed in the land cover change areas of the land cover  
206 scenarios). The results were entirely consistent with the results that were  
207 obtained by using one parameter set (see the supplementary material).  
208 Thus, based on GLUE results obtained by Gao et al. (2016) using SD-  
209 TOPMODEL, the one well-performing parameter set chosen was  
210 appropriate.

211 The velocity parameter of overland flow was derived from an empirical study  
212 of Holden et al. (2008) in a UK blanket peatland catchment, in which  
213 overland flow was investigated for different vegetation types, slopes and flow  
214 depths. It was found that mean velocity of overland flow and Darcy-  
215 Weisbach roughness could be based on a single parameter for each typical  
216 land-surface cover (see Section 2.4).

217

218 **2.3 Designed rainfall events and land-cover scenarios**

219 To investigate impacts of rainfall intensities on hydrographs in flood events,  
220 20 mm, 30 mm, 40 mm and 50 mm storm events (1 hr duration) were  
221 applied as the modelled inputs of precipitation. These values were based on  
222 an investigation of extreme events which were realistic for the study region.  
223 A 1-hr 20 mm hr<sup>-1</sup> rainfall event is approximately equivalent to a 10-year  
224 return period event estimated from the empirical frequency of summer  
225 rainfall events in the study catchment (from 1993 to 2009). The 1-hr 50 mm  
226 event is the largest 1-hr rainfall observed in the period for which rainfall data  
227 are available in the catchment. For each rainfall depth, a series of temporal  
228 precipitation patterns were designed, i.e. uniform profile, late peak profile  
229 (more intense toward the end of the storm), early peak profile (more intense  
230 at the start of the storm) and middle peak profile (Figure 2).

231

232 Land-cover scenarios employed in the modelling experiments included a  
233 baseline scenario, two sets of land-cover change scenarios, and a set of  
234 bare peat soil and revegetation scenarios. The baseline land-cover scenario  
235 assumed that all of the catchment was covered by *Eriophorum* which, in fact,  
236 dominates the vegetation cover of the Trout Beck catchment.

237

238 The three scenario sets of land-cover change - the slope position scenarios,  
239 the riparian zone scenarios and the steep-gentle slope scenarios (see Figure  
240 3 a to g) - were selected to provide a range of different spatial configurations  
241 and to test commonly held assumptions about the spatial sensitivity of  
242 catchment cover for flood risk. These three main sets of scenarios were  
243 investigated in the modelling study of Gao et al. (2016) under a 20 mm storm  
244 event. Hence, by adopting the same main land-cover change scenarios we  
245 can compare our results to those in that earlier study. For the riparian zone  
246 scenarios, the river channel networks were defined with three different  
247 thresholds of accumulative upslope areas (i.e. 250 cells, 1000 cells, and  
248 3000 cells). In a peatland catchment, the network of river channels can be  
249 complicated by headwater gullies with only intermittent flow. The channel  
250 network can be defined with different thresholds of accumulative upslope  
251 areas. A high threshold will produce a short downstream channel network  
252 and a low threshold will define an extended and upslope-connected channel  
253 network. Considering the resolution of the DEM data (20 m x 20 m) used in  
254 this study and avoiding an unrealistically large area of hillslopes being



255 covered by riparian zones, 1.2 km<sup>2</sup> (3000 cell), 0.4 km<sup>2</sup> (1000 cell), and 0.1  
256 km<sup>2</sup> (250 cell) cumulative upslope areas were selected as thresholds to  
257 organize the riparian zone scenarios. The steepest 10 % of the catchment  
258 area and the flattest 10 % of the catchment were selected for land-cover  
259 change in the steep or gentle slope scenarios. The final land-cover change  
260 scenario – revegetation of bare peat areas - involved data from a field  
261 survey in 2012 by North Pennines Area of Outstanding Natural Beauty  
262 Partnership (Figure 3h) which mapped areas of bare peat that the  
263 Partnership seek to revegetate. In practice these maps overestimate bare  
264 peat coverage, as they broadly define areas with high concentrations of bare  
265 peat, rather than wholly unvegetated areas.

266

267 Two land-cover types, bare soil and *Sphagnum*, were used to replace the  
268 *Eriophorum* cover respectively on the target sites of the catchment in each  
269 scenario to represent possible vegetation loss and restoration. This is a  
270 realistic approach as many upland blanket peatlands have become eroded  
271 and bare (Evans and Warburton, 2007) and restoration agencies seek to  
272 revegetate these systems, often by encouraging *Sphagnum* regeneration  
273 (Parry et al., 2014). For the revegetation of bare peat scenario, change for  
274 these areas in our model involved revegetation with either *Eriophorum* or  
275 *Sphagnum*. In all land-cover scenarios, the parameter of overland flow  
276 velocity ( $k_v$ ) was set to five times greater on bare peat areas than on  
277 *Eriophorum* while the velocity parameter on *Sphagnum* areas was half that  
278 of the *Eriophorum* areas. This relationship between the overland flow  
279 velocity parameters (an inverse roughness parameter) of *Sphagnum*,  
280 *Eriophorum*, and bare peat is based on the field study of (Holden et al.,  
281 2008).

282

283 For each land-cover scenario, except the revegetation of bare peat scenario,  
284 land-cover change area was set to be 10 % of the catchment. For the real  
285 bare peat scenario, 9.7 % of the catchment was mapped as bare and  
286 therefore this 9.7 % of the catchment was modified in the associated  
287 revegetation scenarios. For the baseline land-cover scenario, all four rainfall  
288 patterns for each rainfall depth were used as the input in model runs.  
289 However, to save computing time, all four rainfall patterns, for the 30 mm  
290 rainfall depth only, were employed for all land-cover change scenario  
291 modelling.

292

## 293 **2.4 Modelling runs**

294 The DEM grid cell used in the study was 20m x 20m. The time step used in  
295 the scenario modelling runs was 0.1 hr in order to help identify minor  
296 differences in peak timings and size between scenario results. For each  
297 scenario, it was assumed that there was no overland flow on hillslopes at the  
298 first time step but that 90% of cells were saturated. At the start of each run  
299 there was a model warming-up stage of 10 time steps (i.e. 1 hour). This was  
300 sufficient as the moisture deficit of every cell is derived from the starting  
301 runoff at the catchment outlet based on its topographic index. The model  
302 was set up with a wet antecedent condition at the beginning of the warming-  
303 up stage, with 90% of the catchment being saturated and no overland flow  
304 occurring on hillslopes. Therefore 10 time steps were enough to produce an  
305 equilibrium condition for rainfall-runoff simulation. Then one of the designed  
306 rainfalls (10 time steps long) began followed by another 80 time steps  
307 without any rainfall. However, the example figures presented in the results  
308 section below focus on the key flood responses during the first 60 time steps  
309 rather than all additional time-steps of the recession limb.

310

## 311 **3 Results**

### 312 **3.1 River flow peaks with land-cover change under different rainfall** 313 **intensities (uniform profile)**

314 Under different rainfall intensities, the bare peat scenarios had earlier and  
315 increased flow peaks in the river channel compared with the baseline  
316 scenario; conversely the scenarios with dense vegetation cover (i.e.  
317 *Sphagnum*) delayed and reduced river flow peaks (Table 1).

#### 318 ***Riparian strips***

319 In terms of strip position on hillslopes, the riparian bare peat strips created  
320 the earliest and highest river flow peaks compared with mid-slope and  
321 headwater bare peat strips (see Table 1) in the different rainfall events (20  
322 mm hr<sup>-1</sup> to 50 mm hr<sup>-1</sup>). *Sphagnum* cover on the riparian strips created later  
323 and lower flow peaks than on mid-slope and headwater strips. For riparian  
324 strips located based on different thresholds of accumulative upslope  
325 drainage area, bare peat surrounding river channels defined by low  
326 thresholds (250 cells, 0.1 km<sup>2</sup>) had earlier and higher river flow peaks than

327 riparian strips surrounding high-threshold river channels (3000 cells, 1.2  
328 km<sup>2</sup>). *Sphagnum* cover on thinner riparian strips created later and lower river  
329 flow peaks than on thicker strips covering the same proportion of the  
330 catchment. Figure 4 presents the distribution maps of overland flow velocity  
331 and depth for the baseline scenario, the 250-cell bare peat riparian strip  
332 scenario, and the 250-cell *Sphagnum* riparian strip scenario at time step 21  
333 after 30 mm uniform rainfall. There was larger overland flow velocity on the  
334 bare peat riparian regions than on the two vegetation covers; while more  
335 water was retained alongside water courses for the *Sphagnum* riparian strip  
336 scenario than the other scenarios.

### 337 ***Gentle and steep slopes***

338 For the scenario sets of land-cover change on gentle slope areas or steep  
339 slope areas, the results showed that bare peat on gentle slopes induced  
340 higher and earlier flow peaks than bare peat on steep slopes while  
341 *Sphagnum* on gentle slopes produced lower and later peaks than those on  
342 steep slopes (Table 1).

### 343 ***Revegetation of bare peat patches***

344 Revegetating current bare peat areas reduced and delayed river flow peaks  
345 under each rainfall intensity, while revegetation with *Sphagnum* reduced  
346 peak flow more than with *Eriophorum* (Table 1).

### 347 ***Rainfall intensity***

348 For most scenario sets under higher rainfall intensities, the relative (%)  
349 differences between peak flow rates for different land-cover change  
350 scenarios (relative to the peaks of the baseline scenario) were smaller than  
351 under lighter rainfall intensities (Table 1). For example, bare peat on the  
352 riparian strips along channels defined by 3000 upslope drainage cells  
353 increased flood peaks by 7.5% at 20 mm hr<sup>-1</sup> but only 2.3 % at 50 mm hr<sup>-1</sup>;  
354 *Sphagnum* cover on the same strips reduced flood peaks by 6.3 % at 20 mm  
355 hr<sup>-1</sup> rainfalls to 3.3% at 50 mm hr<sup>-1</sup> rainfalls. However, the absolute difference  
356 of the flow peaks between the land-cover change scenarios and the baseline  
357 scenarios increased (non-linearly) as rainfall intensity became greater.  
358 Decreases in flow peaks were 2.6 m<sup>3</sup> s<sup>-1</sup> for 3000 cell *Sphagnum* strips  
359 compared with baseline at 20 mm hr<sup>-1</sup> rainfall but 4.7 m<sup>3</sup> s<sup>-1</sup> at 50 mm hr<sup>-1</sup>  
360 rainfall. Figure 5 presents a scenario comparison including the 250-cell  
361 riparian scenario (Figure 3c), the gentle slope scenario (Figure 3g), and the  
362 headwater scenario (Figure 3e) to show the impacts on peak flow under  
363 different rainfall intensities.

364

### 365 **3.2 River flow peaks under non-uniform rainfall events**

366 For the baseline land-cover scenario, all rainfall patterns with non-uniform  
367 profiles increased river flow peaks and changed peak timings compared with  
368 the corresponding uniform-profile events with the same total rainfall. The  
369 resulting hydrographs are shown in Figure 6. The early rainfall peak profile  
370 resulted in an earlier but lower river flow peak compared with the middle and  
371 late peak profiles in each rainfall depth scenario. The flow peak of the middle  
372 peak profile was later than the early rainfall peak profile but earlier than the  
373 late peak profile in each scenario. The late peak profiles created higher river  
374 flow peaks than the middle profiles under all rainfall events, even though  
375 results were close for the 50 mm rainfall event. Taking the 20 mm set as an  
376 example (Figure 6a), non-uniform rainfall patterns increased flow peaks by  
377 1.4%, 5.9% and 7.5% respectively for the early peak profile, the middle peak  
378 profile, and the late peak profile, compared with the uniform rainfall profile.  
379 The relative differences of river flow peaks under uniform and non-uniform  
380 rainfalls were greater with increased precipitation intensity. For example,  
381 during the 50 mm rainfall event (Figure 6d), the late, middle, and early  
382 rainfall profiles had 3.9%, 19.0% and 19.6% higher river flow peaks than the  
383 uniform rainfall profile, which are much larger differences than for lesser  
384 rainfall depths.

385

### 386 **3.3 River flow peaks with land-cover change under non-uniform** 387 **rainfall events**

388 Land-cover change under storms with non-uniform temporal precipitation  
389 profiles generally resulted in larger impacts on river flow peaks compared  
390 with those storms with uniform rainfall.

#### 391 ***Riparian strips***

392 Under rainfalls with different temporal patterns, the riparian bare peat strip  
393 created earlier and higher river flow peaks than the mid-slope and  
394 headwater bare peat strips. Conversely, *Sphagnum* cover on the riparian  
395 strips resulted in later and lower flow peaks than on the mid-slope strips and  
396 the headwater strips. However, the flow peaks produced by having mid-  
397 slope strips of land-cover change were quite similar to the peaks of riparian  
398 strips under the non-uniform profile rainfalls. For example, under the early  
399 peak rainfall the differences of the *Sphagnum* riparian strip and the

400 *Sphagnum* mid-slope strip peaks (compared with the peak of the baseline  
401 scenario) were 4.7% ( $3.51 \text{ m}^3 \text{ s}^{-1}$ ) and 3.4% ( $2.56 \text{ m}^3 \text{ s}^{-1}$ ) (Table 2).

402 For the different riparian strip scenarios, land-cover change on the 250-cell  
403 riparian strip had a larger impact on river flow peaks than the 1000-cell and  
404 3000-cell riparian strips (Table 2). For example, under the late peak rainfall,  
405 bare peat on the 250-cell riparian strip increased the river flow peak by  
406 11.4% ( $9.58 \text{ m}^3 \text{ s}^{-1}$ ), while the 1000-cell and 3000-cell riparian strips were  
407 associated with 9.1% ( $7.67 \text{ m}^3 \text{ s}^{-1}$ ) and 4.2% ( $3.51 \text{ m}^3 \text{ s}^{-1}$ ) flow peak  
408 increases. Changing to *Sphagnum* cover on the 250-cell riparian strip  
409 created an 11.7% ( $9.90 \text{ m}^3 \text{ s}^{-1}$ ) reduction of river flow peak, which was more  
410 than the 11.0% ( $9.26 \text{ m}^3 \text{ s}^{-1}$ ) reduction for the 1000-cell riparian strip and the  
411 7.6% ( $6.39 \text{ m}^3 \text{ s}^{-1}$ ) reduction for the 3000-cell riparian strip.

412

#### 413 ***Gentle and steep slopes***

414 Under all non-uniform rainfall events, bare peat on the gentle slope areas  
415 gave much higher river flow peaks than that on steep slopes; conversely  
416 *Sphagnum* on gentle slopes made lower flow peaks than steep slopes  
417 (Figure 7). River flow peaks were increased by bare peat on steep slopes  
418 and gentle slopes by 3.9% ( $2.87 \text{ m}^3 \text{ s}^{-1}$ ) and 8.6% ( $6.39 \text{ m}^3 \text{ s}^{-1}$ ) under the  
419 early peak storm, by 3.1% ( $2.56 \text{ m}^3 \text{ s}^{-1}$ ) and 10.9% ( $8.94 \text{ m}^3 \text{ s}^{-1}$ ) under the  
420 middle peak storm, and by 1.1% ( $0.96 \text{ m}^3 \text{ s}^{-1}$ ) and 8.0% ( $6.71 \text{ m}^3 \text{ s}^{-1}$ )  
421 respectively under the late peak storm compared with the baseline scenario  
422 in each case. *Sphagnum* cover on steep slopes and gentle slopes  
423 decreased river flow peaks by 1.7% ( $1.28 \text{ m}^3 \text{ s}^{-1}$ ) and 8.1% ( $6.07 \text{ m}^3 \text{ s}^{-1}$ )  
424 under the early peak storm, by 1.2% ( $0.96 \text{ m}^3 \text{ s}^{-1}$ ) and 9.0% ( $7.36 \text{ m}^3 \text{ s}^{-1}$ )  
425 under the middle peak storm, and by 5.7% ( $4.79 \text{ m}^3 \text{ s}^{-1}$ ) and 11.4% ( $9.58 \text{ m}^3$   
426  $\text{s}^{-1}$ ) under the late peak storm respectively.

427

#### 428 ***Revegetation on real bare peat areas***

429 Revegetation on the real bare peat areas decreased river flow peaks under  
430 storms for all precipitation profiles. The flow peaks were reduced by  
431 *Eriophorum* cover (3.7 %,  $2.87 \text{ m}^3 \text{ s}^{-1}$ ) and *Sphagnum* cover (7.4 %,  $5.75 \text{ m}^3$   
432  $\text{s}^{-1}$ ) under the early peak rainfall compared with the baseline bare peat  
433 cover. Under the middle peak rainfall the *Sphagnum*-induced peak flow  
434 reductions were 5.5 % ( $4.79 \text{ m}^3 \text{ s}^{-1}$ ) and 7.4 % ( $6.39 \text{ m}^3 \text{ s}^{-1}$ ), while they were

435 and 0.8 % ( $0.64 \text{ m}^3 \text{ s}^{-1}$ ) and 5.3 % ( $4.47 \text{ m}^3 \text{ s}^{-1}$ ) respectively under the late  
436 peak rainfall (Table 2).

437

438 A scenario comparison of the impacts on peak flow with different rainfall  
439 patterns is illustrated in Figure 8. Bare peat in the riparian areas and the  
440 flattest areas under the 30 mm late peak rainfall increased river flow peaks  
441 more than the other rainfall patterns; while revegetation in these areas with  
442 *sphagnum* under the 30 mm late peak rainfall made more river flow peak  
443 reduction than the other rainfall patterns.

444

## 445 **4 Discussion**

### 446 **4.1 Impacts of land-cover change on river flow peaks under varying** 447 **rainfall intensities**

#### 448 **4.1.1 Relative and absolute change in flow peaks**

449 As rainfall intensity increased from  $20 \text{ mm hr}^{-1}$  to  $50 \text{ mm hr}^{-1}$ , the relative  
450 changes of the river flow peaks decreased for most of the land-cover change  
451 scenarios compared with the baseline scenario but the absolute changes of  
452 those peaks became larger (especially for rainfall increasing from 20 mm to  
453 40 mm), which matters for flooding. Interestingly, the absolute change in  
454 peaks between land-cover scenarios for 50 mm rainfall events were  
455 sometimes similar to those for 40 mm rainfall events (Table 1), potentially  
456 suggesting there is an upper limit for rainfall event size in enhancing land-  
457 cover change impacts on flood peaks. However, as the results showed that  
458 loss of vegetation cover can increase flood peaks by a larger absolute value  
459 in heavier rainfall events than in smaller storms, and conversely revegetation  
460 can also reduce flood peaks by a larger absolute amount in heavier storms  
461 than in smaller ones, revegetation still benefits flood risk attenuation even  
462 under extreme storm events. This finding is not in line with research on non-  
463 wetland soils where forest impacts on floods have been studied (e.g.  
464 Bathurst et al., 2011a; Bathurst et al., 2011b). These forest studies  
465 suggested that effects on flood peaks of either afforestation or deforestation  
466 were most evident for small to moderate rainfall events but not for extreme  
467 events. It may be that in forest soils enhanced soil water storage effects are  
468 the dominant factor for small and medium storms but this storage becomes  
469 overwhelmed in large storms. For blanket peatlands, there is very little soil  
470 water storage even after dry periods and saturation quickly occurs. Thus the

471 key effect is from slowing the velocity of overland flow. A dense carpet of  
472 *Sphagnum* often > 10 cm thick, can effectively slow flows across the entire  
473 hillslope being important even for the largest storms with deepest sheetflow.

474

475 Land-cover change on riparian zones (hilltoe areas) had more impact on  
476 stream flow peaks than cover change on other areas of hillslopes (e.g. mid-  
477 slope and headwater areas) under all rainfall intensities tested. However, the  
478 impact of land-cover change on headwater regions almost approached that  
479 of the 3000 cell-defined riparian regions under the 50 mm storm. This is  
480 likely to be due to the slightly reduced effect of surface roughness on  
481 overland flow movement under large overland flow depths.

482

#### 483 **4.1.2 Riparian strips**

484 Riparian strip impacts on river flow peaks were close to those of the mid-  
485 slope and headwater buffer strips under the largest rainfall intensity tested.  
486 Gao et al. (2016) indicated that the impact of the converging shape of  
487 natural catchments, and the accompanying overland flow concentration,  
488 makes riparian zones and hilltoe areas more efficient for affecting overland  
489 flow movement. However, under higher rainfall intensity, overland flow  
490 accumulation on the lower areas of hillslopes could lead to large overland  
491 flow depths, which may weaken the efficiency of the surface roughness  
492 effect on overland flow movement in riparian areas. Thus, the peak flow  
493 differences between the riparian strip scenarios and the other scenarios  
494 became small under high rainfall intensities.

495 Considering that riparian buffer strips surround stream channels with  
496 different thresholds of accumulation area, land-cover change on the thin but  
497 branching riparian buffer strips (based on channels with low accumulative  
498 area threshold) had a larger impact on river flow peaks even under high  
499 rainfall intensities (50 mm hr<sup>-1</sup> in this study). This result supports the finding  
500 of Gao et al. (2016), in which it was indicated that thicker riparian strips  
501 contain outer cells that are away from stream channel, and have lower  
502 efficiency in affecting river flow than that of thinner riparian strips. In storm  
503 events with high precipitation intensities, revegetation on the branching  
504 riparian strips still produced more benefits for flood risk control than  
505 revegetation on thicker riparian strips or on other areas in the catchment. For  
506 example, *Sphagnum* cover on the 250-cell channel riparian strip in the Trout  
507 Beck catchment had considerable impact on river flow peak under the 40

508 mm hr<sup>-1</sup> and 50 mm hr<sup>-1</sup> rainfall events (6.4% and 5.6% reductions). This  
509 may be because, even for the rainfall intensity of 50 mm hr<sup>-1</sup>, the impact of  
510 land-cover change in upstream riparian areas on low-depth overland flow is  
511 still efficient compared with that of the downstream riparian zones where  
512 flow depths will be greater.

513

#### 514 **4.1.3 Slope**

515 Land-cover change on flat slopes influence flow peaks more than on steep  
516 locations in this catchment under all rainfall intensities tested. Impacts of  
517 land-cover change on flat slopes on river flow peaks are strong even under  
518 high rainfall intensities. This indicates that revegetation on gentle slopes can  
519 provide reliable benefits to flood attenuation no matter what the temporal  
520 rainfall pattern is. In practice, there could be a high priority towards  
521 revegetation on gentle slope areas in target catchments.

522

#### 523 **4.1.4 Revegetation**

524 Reduction of river flow peaks induced by revegetation on real bare peat  
525 areas in the study catchment was quite limited and decreased (for both the  
526 absolute and relative changes) with rainfall intensity. This is because most of  
527 the bare patches were not on the sensitive areas of the catchment that  
528 impact overland flow movement and concentration efficiently (e.g. riparian  
529 areas and flat slopes). Revegetation simply on bare soil patches without  
530 spatial planning could have little value for flood peak attenuation in extreme  
531 storm events.

532

### 533 **4.2 Impacts of temporal rainfall patterns on river flow peaks**

534 Temporal rainfall patterns have impacts on downstream flood peaks in the  
535 Trout Beck peatland catchment. The time differences of the flow peaks  
536 under different rainfall patterns (with identical total rainfall depth) were  
537 expected but the changes of the flow peak sizes were also considerable.  
538 Previous studies (presented in section 1 of this paper) suggested that the  
539 decay of soil infiltration capacity and/or the formation of soil surface sealing  
540 during storm events lead to peak flow rate differences under different rainfall  
541 patterns. Early peak rainfall, by first filling the pore spaces in the soil, could  
542 produce less overland flow to form a lower flow peak at the outlet of the  
543 catchment compared with the middle and late peak rainfall patterns which



544 occur after the saturation has already been established in the initial part of  
545 the storm. However, these mechanisms are not the case in a peatland  
546 catchment which is well covered by vegetation and dominated by rapid  
547 development of saturation-excess overland flow. The soil moisture deficit of  
548 the whole catchment in this study was set to be very small at the start of the  
549 model runs (less than 0.1 mm depth for the whole catchment). The  
550 difference between the flood peaks was much larger than this deficit. For  
551 example, the peak difference was 0.5 mm per 6 min under 40 mm rainfall  
552 and 0.8 mm per 6 min under 50 mm rainfall. Thus the soil moisture deficit  
553 cannot explain the magnitude of difference between flood peaks.  
554 Furthermore, flow peaks for the middle peak rainfall patterns were also lower  
555 than those of the late peak rainfall patterns.

556

557 Changes to precipitation time series induce changes in overland flow  
558 production at every location in the catchment, and consequently overland  
559 flow movement on hillslopes could also be altered to change river flow  
560 peaks. For the early peak rainfall pattern, precipitation with a high intensity at  
561 the beginning of the rainfall event generated overland flow which had a large  
562 flow depth and transport velocity on hillslopes, so surface water travels  
563 downslope relatively fast. Additional precipitation falling onto the surface  
564 water increased water depth and accelerated overland flow delivery on  
565 hillslopes. However, this acceleration of overland flow movement on  
566 hillslopes (particularly on headwater areas) becomes weaker for smaller  
567 rainfall intensities in proceeding time steps after the peak rainfall has  
568 occurred. In downslope areas, however, the delivery and concentration of  
569 overland flow is still quite fast in these follow-up time steps due to the  
570 overland flow which was produced in the early time steps by intensive  
571 precipitation. Thus, there seemed to be a split of overland flow movement on  
572 hillslopes when the early peak rainfall pattern tended to generate obtuse and  
573 wide hydrographs at the catchment outlet. In contrast, for the late peak  
574 rainfall patterns, initially low precipitation produced shallow surface water  
575 and slow overland flow; while in the following time steps the increasing  
576 precipitation produced deep and fast overland flow which was 'chasing' the  
577 downslope overland flow generated earlier. Therefore, it seems that late  
578 peak rainfall patterns were more likely to create sharp and thin river flow  
579 peaks than the early peak rainfall distributions. For the middle peak patterns,  
580 river flow peaks were quite close to the flow peaks under the late peak  
581 rainfalls, particularly under large rainfall depths. This may be because the

582 concentration of rainfall around the rainfall peak of the middle peak pattern  
583 was larger than that of the early peak pattern (e.g. for the 50 mm events the  
584 rainfall depth of the four middle steps in the middle rainfall pattern was 33.5  
585 mm and the depth of the early four steps in the early rainfall pattern was 32  
586 mm). The 'chasing' effects in overland flow movement (same for the late  
587 peak rainfall patterns above) were shorter but faster than those under the  
588 late peak rainfall patterns in the first half of the rainfall period due to the  
589 rapider increase in rainfall intensity during the first half than during rainfall  
590 with the late peak pattern (Figure 2). Even though rainfall intensity  
591 decreased in the second half of the period, river flow peaks under the middle  
592 peak patterns were still high and the difference between river flow peaks of  
593 the early and middle peak rainfall patterns was greater than that between the  
594 middle and late peak rainfall patterns.

#### 595 **4.3 Impacts of land cover change on river flow peaks under different** 596 **temporal rainfall patterns**

597 Temporal rainfall patterns affected impacts of land-cover change on river  
598 flow peaks. Non-uniform rainfall patterns magnified the impact of land-cover  
599 change on river flow peaks (for both absolute and relative changes)  
600 compared with the uniform rainfall pattern with identical total precipitation  
601 depth. Such changes were particularly magnified for land-cover change on  
602 sensitive areas (i.e. riparian zones and flat slopes). Among the non-uniform  
603 rainfall patterns, land-cover change on the sensitive areas under the middle  
604 and late peak rainfalls had greater impacts on river flow peaks (for both  
605 relative and absolute differences compared with the baseline land cover)  
606 than the early peak rainfall. Under a particular timed pattern of precipitation,  
607 there is a particular variation of the overland flow vector field in the  
608 catchment including spatial and temporal change of surface water delivery. It  
609 could be inferred that the sensitive areas are the key areas for overland flow  
610 delivery under the middle and late peak rainfall patterns. This means that  
611 protection and restoration of vegetation cover on these areas could bring  
612 greater reduction of flood risk under these rainfall patterns.

613

#### 614 **4.4 Sensitivity of locations in a catchment to river flow peaks under** 615 **varying rainfall characteristics**

616 The sensitivity of manipulating a location in a catchment to drive change in  
617 river flow peaks varies with rainfall characteristics. For instance, bare peat  
618 on a mid-slope strip (covering 10% area of the catchment) created a higher

619 river flow peak under the 30 mm early peak rainfall profile, than bare peat on  
620 riparian regions. Further, the 'most' sensitive regions for impacting river flow  
621 peaks also change under different rainfall depths and patterns. For example,  
622 the mid-slope bare strip increased river flow peak by 6.8% which was  
623 greater than bare peat on the 3000-cell riparian strip (5.1%). Thus, a new  
624 algorithm will be needed to directly locate the most sensitive areas in a  
625 catchment under different rainfall characteristics. These most sensitive  
626 locations would inform a new understanding of flood risk and its attenuation  
627 at a catchment scale. There would be a type of 'worst case scenario' rainfall  
628 pattern, given a certain rainfall depth for a particular catchment, which could  
629 potentially interact with the topography and land-cover of the catchment. Under  
630 the worst rainfall patterns, vegetation degradation and loss could bring  
631 higher river flow peaks and larger flood risk than for other rainfall patterns  
632 with same total rainfall; while revegetation would result in a greater reduction  
633 to river flow peaks. Hence, a new method is needed to identify generalized  
634 sensitive regions with good consideration of the characteristics of the local  
635 storm events based on the historical record or future climate scenarios for  
636 rainfall in the target catchment.

637 The results of our sensitivity study were based on a small scale catchment,  
638 in which hillslope overland flow responses to rainfall was the key component  
639 impacted by land cover change. However, for a larger scale catchment,  
640 channel flow routing components in the river network may be not negligible  
641 (e.g. Bovolo and Bathurst, 2012) and should be considered in future larger  
642 scale studies.

643

## 644 ***5 Conclusion***

645 Using SD-TOPMODEL, our work focussed on a case study catchment  
646 demonstrating that there are strong effects on flood peaks of rainfall intensity  
647 distributions during a storm and strong interaction effects of these rainfall  
648 patterns with spatial land cover configurations. In that sense we believe our  
649 findings are generalizable, at least to the case of blanket peat covered  
650 catchments that are dominated by shallow water tables and widespread  
651 saturation-excess overland flow response. However, future studies could  
652 examine the impact of different catchment sizes and topographic  
653 configurations on these patterns.

654

655 Figure 9 summarises the effects on flood peaks that we found for the  
656 interaction between rainfall intensity, rainfall pattern, and land cover location.  
657 The interaction effects are strong with land-cover change effects being  
658 mediated or enhanced by temporal rainfall patterns in non-linear ways.  
659 Figure 9 illustrates how under the same rainfall depth, non-uniform rainfall  
660 (including early, middle and late rainfall peak patterns) produced higher river  
661 flow peaks than uniform rainfall. Late peak rainfall patterns resulted in the  
662 highest river flow peaks, while middle peak patterns created larger river flow  
663 peaks than early peak patterns. These differences occur because varying  
664 rainfall patterns changed the conditions of overland flow delivery and  
665 concentration on hillslopes.

666

667 With different rainfall characteristics, land-cover change impacts on river flow  
668 peaks were generally in line with the findings of Gao et al. (2016) which was  
669 conducted under a single uniform rainfall (i.e. the 1-hr 20 mm hr<sup>-1</sup> rainfall).  
670 However, the relative differences in effect on flood peaks between the land-  
671 cover change scenario and the baseline scenario became closer as rainfall  
672 intensity increased (i.e. 20 mm hr<sup>-1</sup> to 50 mm hr<sup>-1</sup>, keeping the rainfall  
673 duration as 1 hour), while the absolute change became larger with increased  
674 rainfall intensity. For non-uniform rainfall, land-cover change impacts on river  
675 flow peaks were increased in terms of both absolute and relative changes  
676 compared with the uniform rainfall patterns, especially for the cover change  
677 on the most sensitive areas - riparian zones and gentle gradient slopes.  
678 Moreover, land-cover change on sensitive areas under middle and late peak  
679 rainfalls resulted in greater river flow peak changes relative to the land-cover  
680 baseline than the flow peak changes under the early peak rainfall. For  
681 vegetation restoration in upland peat catchments, the best action is to  
682 provide good buffer strips along the waterways, taking particular care to treat  
683 flatter areas and any bare patches, in which the more the better but a 10%  
684 areal treatment is well worth doing. Under different rainfall characteristics  
685 (e.g. intensities and temporal patterns), land-cover change on a same region  
686 in a catchment may have very different impacts on river flow peaks.

687

688 ***Acknowledgements***

689 We thank the Environment Agency of England for provision of discharge and  
690 precipitation data for the model parameterization. We thank the North  
691 Pennines AONB Partnership for their bare peat map.

692

693 ***References***

694

- 695 Ballard, C.E., McIntyre, N., Wheeler, H.S., Holden, J., Wallage, Z.E., 2011.  
696 Hydrological modelling of drained blanket peatland. *J. Hydrol.*, 407(1-  
697 4): 81-93. DOI:10.1016/j.jhydrol.2011.07.005
- 698 Bathurst, J.C. et al., 2011a. Forest impact on floods due to extreme rainfall  
699 and snowmelt in four Latin American environments 2: Model analysis.  
700 *J. Hydrol.*, 400(3-4): 292-304. DOI:10.1016/j.jhydrol.2010.09.001
- 701 Bathurst, J.C. et al., 2011b. Forest impact on floods due to extreme rainfall  
702 and snowmelt in four Latin American environments 1: Field data  
703 analysis. *J. Hydrol.*, 400(3-4): 281-291.  
704 DOI:10.1016/j.jhydrol.2010.11.044
- 705 Beven, K., Binley, A., 1992. The future of distributed models - model  
706 calibration and uncertainty prediction. *Hydrol. Process.*, 6(3): 279-  
707 298. DOI:10.1002/hyp.3360060305
- 708 Beven, K.J., Kirkby, M.J., 1979. A physically-based variable contributing  
709 area model of basin hydrology. *Hydrol. Sci. Bull.*, 24: 43-69.
- 710 Bovolo, C.I., Bathurst, J.C., 2012. Modelling catchment-scale shallow  
711 landslide occurrence and sediment yield as a function of rainfall return  
712 period. *Hydrol. Process.*, 26(4): 579-596. DOI:10.1002/hyp.8158
- 713 Dadson, S.J. et al., 2017. A restatement of the natural science evidence  
714 concerning catchment-based 'natural' flood management in the UK.  
715 *Proceedings of the Royal Society a-Mathematical Physical and*  
716 *Engineering Sciences*, 473(2199): 19. DOI:10.1098/rspa.2016.0706
- 717 Dolsak, D., Bezak, N., Sraj, M., 2016. Temporal characteristics of rainfall  
718 events under three climate types in Slovenia. *J. Hydrol.*, 541: 1395-  
719 1405. DOI:10.1016/j.jhydrol.2016.08.047
- 720 Dunkerley, D., 2012. Effects of rainfall intensity fluctuations on infiltration and  
721 runoff: rainfall simulation on dryland soils, Fowlers Gap, Australia.  
722 *Hydrol. Process.*, 26(15): 2211-2224. DOI:10.1002/hyp.8317
- 723 Dunkerley, D., 2014. Stemflow production and intrastorm rainfall intensity  
724 variation: an experimental analysis using laboratory rainfall  
725 simulation. *Earth Surf. Processes Landforms*, 39(13): 1741-1752.  
726 DOI:10.1002/esp.3555
- 727 Evans, M., Warburton, J., 2007. *The Geomorphology of Upland Peat:*  
728 *Erosion, Form and Landscape Change.* Blackwell Publishing, London.
- 729 Evans, M.G., Burt, T.P., Holden, J., Adamson, J.K., 1999. Runoff generation  
730 and water table fluctuations in blanket peat: evidence from UK data  
731 spanning the dry summer of 1995. *J. Hydrol.*, 221(3-4): 141-160.  
732 DOI:10.1016/s0022-1694(99)00085-2

- 733 Flanagan, D.C., Foster, G.R., Moldenhauer, W.C., 1988. Storm pattern  
734 effect on infiltration, runoff, and erosion. *Transactions of the Asae*,  
735 31(2): 414-420.
- 736 Gallego-Sala, A.V., Prentice, I.C., 2013. Blanket peat biome endangered by  
737 climate change. *Nat. Clim. Change*, 3(2): 152-155.  
738 DOI:10.1038/nclimate1672
- 739 Gao, J., Holden, J., Kirkby, M., 2015. A distributed TOPMODEL for  
740 modelling impacts of land-cover change on river flow in upland  
741 peatland catchments. *Hydrol. Process.*, 29(13): 2867-2879.  
742 DOI:10.1002/hyp.10408
- 743 Gao, J., Holden, J., Kirkby, M., 2016. The impact of land-cover change on  
744 flood peaks in peatland basins. *Water Resour. Res.*, 52: 3477-3492.  
745 DOI:10.1002/2015WR017667
- 746 Gao, J., Holden, J., Kirkby, M., 2017. Modelling impacts of agricultural  
747 practice on flood peaks in upland catchments: an application of the  
748 distributed TOPMODEL. *Hydrol. Process.*, 31(23): 4206-4216.  
749 DOI:10.1002/hyp.11355
- 750 Grayson, R., Holden, J., Rose, R., 2010. Long-term change in storm  
751 hydrographs in response to peatland vegetation change. *J. Hydrol.*,  
752 389(3-4): 336-343. DOI:10.1016/j.jhydrol.2010.06.012
- 753 Holden, J., Burt, T.P., 2002. Infiltration, runoff and sediment production in  
754 blanket peat catchments: implications of field rainfall simulation  
755 experiments. *Hydrol. Process.*, 16(13): 2537-2557.  
756 DOI:10.1002/hyp.1014
- 757 Holden, J., Burt, T.P., 2003. Runoff production in blanket peat covered  
758 catchments. *Water Resour. Res.*, 39(7): 257-271.  
759 DOI:10.1029/2002wr001956
- 760 Holden, J., Evans, M.G., Burt, T.P., Horton, M., 2006. Impact of land  
761 drainage on peatland hydrology. *J. Environ. Qual.*, 35(5): 1764-1778.  
762 DOI:10.2134/jeq2005.0477
- 763 Holden, J. et al., 2008. Overland flow velocity and roughness properties in  
764 peatlands. *Water Resour. Res.*, 44(6): 663-671.  
765 DOI:10.1029/2007wr006052
- 766 Holden, J. et al., 2015. Impact of prescribed burning on blanket peat  
767 hydrology. *Water Resour. Res.*, 51(8): 6472-6484.  
768 DOI:10.1002/2014wr016782
- 769 Holden, J., Rose, R., 2011. Temperature and surface lapse rate change: a  
770 study of the UK's longest upland instrumental record. *Int. J. Climatol.*,  
771 31(6): 907-919. DOI:10.1002/joc.2136
- 772 Holstead, K.L., Kenyon, W., Rouillard, J.J., Hopkins, J., Galan-Diaz, C.,  
773 2017. Natural flood management from the farmer's perspective:  
774 criteria that affect uptake. *J. Flood Risk Manage.*, 10(2): 205-218.  
775 DOI:10.1111/jfr3.12129
- 776 Huff, F.A., 1967. Time distribution of rainfall in heavy storms. *Water Resour.*  
777 *Res.*, 3(4): 1007-1019. DOI:10.1029/WR003i004p01007
- 778 Immirzi, C.P., Maltby, E., Clymo, R.S., 1992. The global status of peatlands  
779 and their role in carbon cycling, Dept Geography, University of Exeter.
- 780 Kirkby, M.J., 1997. TOPMODEL: A personal view. *Hydrol. Process.*, 11(9):  
781 1087-1097. DOI:10.1002/(sici)1099-1085(199707)11:9<1087::aid-  
782 hyp546>3.0.co;2-p

- 783 Lane, S.N., Milledge, D.G., 2013. Impacts of upland open drains upon runoff  
784 generation: a numerical assessment of catchment-scale impacts.  
785 Hydrol. Process., 27(12): 1701-1726. DOI:10.1002/hyp.9285
- 786 Larmola, T. et al., 2010. The role of *Sphagnum* mosses in the methane  
787 cycling of a boreal mire. Ecology, 91(8): 2356-2365. DOI:10.1890/09-  
788 1343.1
- 789 Manley, G., 1942. Meteorological observations on Dun Fell, a mountain  
790 station in northern England. Q. J. R. Meteorolog. Soc., 68: 151-165.
- 791 Parry, L.E., Holden, J., Chapman, P.J., 2014. Restoration of blanket  
792 peatlands. J. Environ. Manage., 133: 193-205.  
793 DOI:<http://dx.doi.org/10.1016/j.jenvman.2013.11.033>
- 794 Price, J.S., 1992. Blanket bog in Newfoundland. Part 2. Hydrological  
795 processes. J. Hydrol., 135(1-4): 103-119. DOI:10.1016/0022-  
796 1694(92)90083-8
- 797 Quinn, P., Beven, K., Chevallier, P., Planchon, O., 1991. The prediction of  
798 hillslope flow paths for distributed hydrological modeling using digital  
799 terrain models. Hydrol. Process., 5(1): 59-79.  
800 DOI:10.1002/hyp.3360050106
- 801 Rogger, M. et al., 2017. Land use change impacts on floods at the  
802 catchment scale: Challenges and opportunities for future research.  
803 Water Resour. Res., 53(7): 5209-5219. DOI:10.1002/2017wr020723
- 804 SEPA, 2011. Natural Flood Management Handbook. Scottish Environmental  
805 Protection Agency, Stirling.
- 806 Willems, P., 2000. Compound intensity/duration/frequency-relationships of  
807 extreme precipitation for two seasons and two storm types. J. Hydrol.,  
808 233(1-4): 189-205. DOI:10.1016/s0022-1694(00)00233-x
- 809 Xu, J.R., Morris, P.J., Liu, J.G., Holden, J., 2018. PEATMAP: Refining  
810 estimates of global peatland distribution based on a meta-analysis.  
811 Catena, 160: 134-140. DOI:10.1016/j.catena.2017.09.010
- 812 Xue, J., Gavin, K., 2007. Effect of rainfall intensity on infiltration into partly  
813 saturated slopes. Geotech. Geol. Eng., 26(2): 199-209.  
814 DOI:10.1007/s10706-007-9157-0
- 815 Yilmaz, A.G., Hossain, I., Perera, B.J.C., 2014. Effect of climate change and  
816 variability on extreme rainfall intensity-frequency-duration  
817 relationships: a case study of Melbourne. Hydrol. Earth Syst. Sci.,  
818 18(10): 4065-4076. DOI:10.5194/hess-18-4065-2014
- 819 Yu, Z.C., Loisel, J., Brosseau, D.P., Beilman, D.W., Hunt, S.J., 2010. Global  
820 peatland dynamics since the Last Glacial Maximum. Geophys. Res.  
821 Lett., 37. DOI:10.1029/2010gl043584

822

823

824 **Tables**

825 Table 1. Modelling results for land-cover scenario impacts on flood peak  
826 under uniform rainfall.

Scenario		Peak flow change compared with the normal scenario			Peak timing change compared with the baseline scenario* (time step)
		Absolute increase		Relative change (%)	
		(mm/6 min)	(m <sup>3</sup> /s)		
20 mm rainfall	Riparian bare strip	0.10	3.13	7.47	1
	Mid-slope bare strip	0.08	2.49	5.95	0
	Headwater bare strip	0.05	1.53	3.66	0
30 mm rainfall	Riparian bare strip	0.09	2.94	3.97	1
	Mid-slope bare strip	0.06	1.98	2.67	1
	Headwater bare strip	0.05	1.66	2.24	1
40 mm rainfall	Riparian bare strip	0.11	3.64	3.38	1
	Mid-slope bare strip	0.09	3.00	2.79	0
	Headwater bare strip	0.07	2.36	2.20	0
50 mm rainfall	Riparian bare strip	0.10	3.26	2.30	0
	Mid-slope bare strip	0.04	1.34	0.95	0
	Headwater bare strip	0.09	2.94	2.08	0
20 mm rainfall	Riparian bare strip (3000)	0.10	3.13	7.47	1
	Riparian bare strip (1000)	0.14	4.41	10.52	1
	Riparian bare strip (250)	0.17	5.37	12.81	1
30 mm rainfall	Riparian bare strip (3000)	0.09	2.94	3.97	1
	Riparian bare strip (1000)	0.18	5.81	7.85	1
	Riparian bare strip (250)	0.21	6.77	9.15	1
40 mm rainfall	Riparian bare strip (3000)	0.11	3.64	3.39	1
	Riparian bare strip (1000)	0.19	6.20	5.76	1
	Riparian bare strip (250)	0.27	8.75	8.14	1
50 mm rainfall	Riparian bare strip (3000)	0.10	3.26	2.30	0
	Riparian bare strip (1000)	0.17	5.49	3.88	0



	Riparian bare strip (250)	0.18	5.81	4.11	0
20 mm rainfall	Riparian <i>Sph.</i> strip	-0.08	-2.62	-6.25	-2
	Mid-slope <i>Sph</i> strip	-0.05	-1.66	-3.96	-1
	Headwater <i>Sph</i> strip	-0.02	-0.70	-1.68	0
30 mm rainfall	Riparian <i>Sph.</i> strip	-0.15	-4.73	-6.39	0
	Mid-slope <i>Sph</i> strip	-0.10	-3.13	-4.23	0
	Headwater <i>Sph</i> strip	-0.06	-1.85	-2.50	0
40 mm rainfall	Riparian <i>Sph.</i> strip	-0.16	-4.98	-4.64	0
	Mid-slope <i>Sph</i> strip	-0.08	-2.43	-2.26	0
	Headwater <i>Sph</i> strip	-0.08	-2.43	-2.26	0
50 mm rainfall	Riparian <i>Sph.</i> strip	-0.15	-4.73	-3.34	-1
	Mid-slope <i>Sph</i> strip	-0.08	-2.49	-1.76	0
	Headwater <i>Sph</i> strip	-0.05	-1.53	-1.08	0
20 mm rainfall	Riparian <i>Sph</i> strip (3000)	-0.08	-2.62	-6.25	-2
	Riparian <i>Sph</i> strip (1000)	-0.11	-3.58	-8.54	-2
	Riparian <i>Sph</i> strip (250)	-0.13	-4.22	-10.06	-2
30 mm rainfall	Riparian <i>Sph</i> strip (3000)	-0.15	-4.73	-6.39	0
	Riparian <i>Sph</i> strip (1000)	-0.19	-6.00	-8.11	-1
	Riparian <i>Sph</i> strip (250)	-0.19	-6.00	-8.11	0
40 mm rainfall	Riparian <i>Sph</i> strip (3000)	-0.16	-4.98	-4.64	0
	Riparian <i>Sph</i> strip (1000)	-0.21	-6.58	-6.12	0
	Riparian <i>Sph</i> strip (250)	-0.22	-6.90	-6.42	-1
50 mm rainfall	Riparian <i>Sph</i> strip (3000)	-0.15	-4.72	-3.34	-1
	Riparian <i>Sph</i> strip (1000)	-0.23	-7.28	-5.15	-1
	Riparian <i>Sph</i> strip (250)	-0.25	-7.92	-5.60	-1
20 mm rainfall	Bare steepest slopes	0.06	1.85	4.42	0
	Bare flattest slopes	0.14	4.41	10.52	1
30 mm rainfall	Bare steepest slopes	0.02	0.70	0.95	1
	Bare flattest slopes	0.18	5.81	7.85	1

40 mm rainfall	Bare steepest slopes	0.08	2.68	2.50	0
	Bare flattest slopes	0.21	6.83	6.36	1
50 mm rainfall	Bare steepest slopes	0.06	1.98	1.40	0
	Bare flattest slopes	0.19	6.13	4.34	0
20 mm rainfall	<i>Sph.</i> steepest slopes	-0.02	-0.70	-1.68	-1
	<i>Sph.</i> flattest slopes	-0.11	-3.58	-8.54	-2
30 mm rainfall	<i>Sph.</i> steepest slopes	-0.04	-1.21	-1.64	0
	<i>Sph.</i> flattest slopes	-0.15	-4.73	-6.39	0
40 mm rainfall	<i>Sph.</i> steepest slopes	-0.06	-1.79	-1.66	0
	<i>Sph.</i> flattest slopes	-0.21	-6.58	-6.12	0
50 mm rainfall	<i>Sph.</i> steepest slopes	-0.05	-1.53	-1.08	0
	<i>Sph.</i> flattest slopes	-0.21	-6.64	-4.70	-1
20 mm rainfall	Revegetation with <i>Erio.</i>	-0.05	-1.53	-3.53	0
	Revegetation with <i>Sph.</i>	-0.09	-2.87	-6.62	-1
30 mm rainfall	Revegetation with <i>Erio.</i>	-0.03	-1.02	-1.36	0
	Revegetation with <i>Sph.</i>	-0.10	-3.19	-4.26	0
40 mm rainfall	Revegetation with <i>Erio.</i>	-0.03	-0.96	-0.87	0
	Revegetation with <i>Sph.</i>	-0.10	-3.19	-2.91	0
50 mm rainfall	Revegetation with <i>Erio.</i>	-0.19	-6.07	-4.18	0
	Revegetation with <i>Sph.</i>	-0.20	-6.39	-4.40	0

827 \* Positive numbers indicate that the peak is earlier than the baseline scenario, while negative

828 numbers indicate the peak is later than the baseline scenario.

829

830 Table 2. Modelling results of land cover scenarios under 30 mm rainfall with  
831 varying temporal patterns.

Land cover scenario		Peak flow change compared with the normal scenario			Peak timing change compared with the baseline scenario * (time step)
		Absolute increase		Relative change (%)	
		(mm/ 6min)	(m <sup>3</sup> /s)		
Uniform	Riparian bare strip	0.09	2.94	3.97	1
	Mid-slope bare strip	0.06	1.98	2.67	1
	Headwater bare strip	0.05	1.66	2.24	1
Early peak	Riparian bare strip	0.12	3.83	5.13	2
	Mid-slope bare strip	0.16	5.11	6.84	1
	Headwater bare strip	0.04	1.27	1.71	1
Middle peak	Riparian bare strip	0.20	6.39	7.81	2
	Mid-slope bare strip	0.17	5.43	6.64	1
	Headwater bare strip	0.09	2.87	3.52	1
Late peak	Riparian bare strip	0.11	3.51	4.17	2
	Mid-slope bare strip	0.08	2.56	3.03	1
	Headwater bare strip	0.03	0.96	1.14	1
Uniform	Riparian strip (3000)	0.09	2.94	3.97	1
	Riparian strip (1000)	0.18	5.81	7.85	1
	Riparian strip (250)	0.21	6.77	9.15	1
Early peak	Riparian bare strip (3000)	0.12	3.83	5.13	2
	Riparian bare strip (1000)	0.19	6.07	8.12	2
	Riparian bare strip (250)	0.26	8.30	11.11	2
Middle peak	Riparian bare strip (3000)	0.20	6.39	7.81	1
	Riparian bare strip (1000)	0.29	9.26	11.33	1
	Riparian bare strip (250)	0.37	11.82	14.45	1
Late peak	Riparian bare strip (3000)	0.11	3.51	4.17	1
	Riparian bare strip (1000)	0.24	7.67	9.09	1
	Riparian bare strip (250)	0.30	9.58	11.36	1
Uniform	Riparian <i>Sph.</i> strip	-0.15	-4.73	-6.39	0

	Mid-slope <i>Sph</i> strip	-0.10	-3.13	-4.23	0
	Headwater <i>Sph</i> strip	-0.06	-1.85	-2.50	0
Early peak	Riparian <i>Sph.</i> strip	-0.11	-3.51	-4.70	0
	Mid-slope <i>Sph</i> strip	-0.08	-2.56	-3.42	0
	Headwater <i>Sph</i> strip	-0.02	-0.64	-0.85	0
Middle peak	Riparian <i>Sph.</i> strip	-0.20	-6.39	-7.81	-1
	Mid-slope <i>Sph</i> strip	-0.10	-3.19	-3.91	0
	Headwater <i>Sph</i> strip	-0.06	-1.92	-2.34	0
Late peak	Riparian <i>Sph.</i> strip	-0.20	-6.39	-7.58	-1
	Mid-slope <i>Sph</i> strip	-0.18	-5.75	-6.82	0
	Headwater <i>Sph</i> strip	0.12	-3.83	-4.55	0
Uniform	Riparian <i>Sph</i> strip (3000)	-0.15	-4.73	-6.39	0
	Riparian <i>Sph</i> strip (1000)	-0.19	-6.00	-8.11	-1
	Riparian <i>Sph</i> strip (250)	-0.19	-6.00	-8.11	0
Early peak	Riparian <i>Sph</i> strip (3000)	-0.11	-3.51	-4.70	0
	Riparian <i>Sph</i> strip (1000)	-0.18	-5.75	-7.69	-1
	Riparian <i>Sph</i> strip (250)	-0.20	-6.39	-8.55	0
Middle peak	Riparian <i>Sph</i> strip (3000)	-0.20	-6.39	-7.81	-1
	Riparian <i>Sph</i> strip (1000)	-0.18	-5.75	-7.03	-1
	Riparian <i>Sph</i> strip (250)	-0.26	-8.30	-10.16	-1
Late peak	Riparian <i>Sph</i> strip (3000)	-0.20	-6.39	-7.58	-1
	Riparian <i>Sph</i> strip (1000)	-0.29	-9.26	-10.99	-1
	Riparian <i>Sph</i> strip (250)	-0.31	-9.90	-11.74	-1
Uniform	Bare steepest slopes	0.02	0.70	0.95	1
	Bare flattest slopes	0.18	5.81	7.85	1
Early peak	Bare steepest slopes	0.09	2.87	3.85	1
	Bare flattest slopes	0.20	6.39	8.55	2
Middle peak	Bare steepest slopes	0.08	2.56	3.12	1
	Bare flattest slopes	0.28	8.94	10.94	0

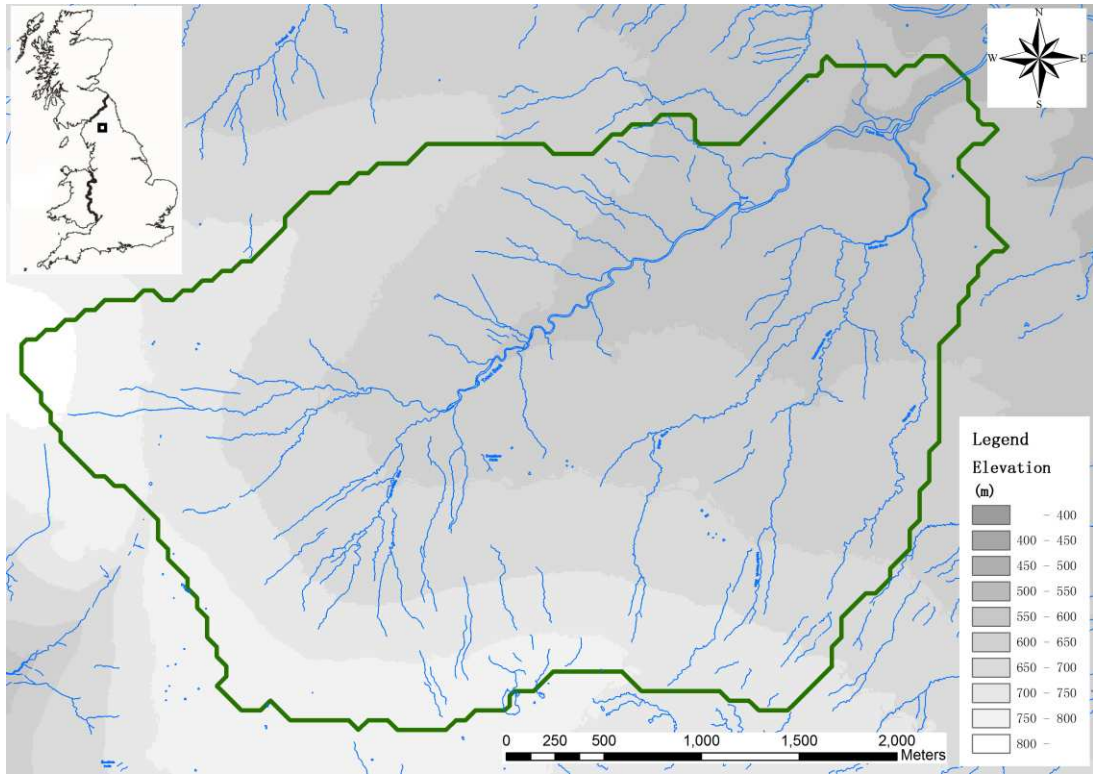
Late peak	Bare steepest slopes	0.03	0.96	1.14	1
	Bare flattest slopes	0.21	6.71	7.95	0
Uniform	<i>Sph.</i> steepest slopes	-0.04	-1.21	-1.64	0
	<i>Sph.</i> flattest slopes	-0.15	-4.73	-6.39	0
Early peak	<i>Sph.</i> steepest slopes	-0.04	-1.28	-1.71	1
	<i>Sph.</i> flattest slopes	-0.19	-6.07	-8.12	0
Middle peak	<i>Sph.</i> steepest slopes	-0.03	-0.96	-1.17	0
	<i>Sph.</i> flattest slopes	-0.23	-7.36	-8.98	-1
Late peak	<i>Sph.</i> steepest slopes	-0.15	-4.79	-5.68	0
	<i>Sph.</i> flattest slopes	-0.30	-9.58	-11.36	-1
Uniform	Revegetation with <i>Erio.</i>	-0.03	-1.02	-1.36	0
	Revegetation with <i>Sph.</i>	-0.10	-3.19	-4.26	0
Early peak	Revegetation with <i>Erio.</i>	-0.09	-2.87	-3.70	-1
	Revegetation with <i>Sph.</i>	-0.18	-5.75	-7.41	0
Middle peak	Revegetation with <i>Erio.</i>	-0.15	-4.79	-5.54	0
	Revegetation with <i>Sph.</i>	-0.20	-6.39	-7.38	0
Late peak	Revegetation with <i>Erio.</i>	-0.02	-0.64	-0.75	0
	Revegetation with <i>Sph.</i>	-0.14	-4.47	-5.26	0

832 \* Positive numbers indicate the peak is earlier than the baseline scenario, while negative numbers

833 indicate the peak is later than the baseline scenario.

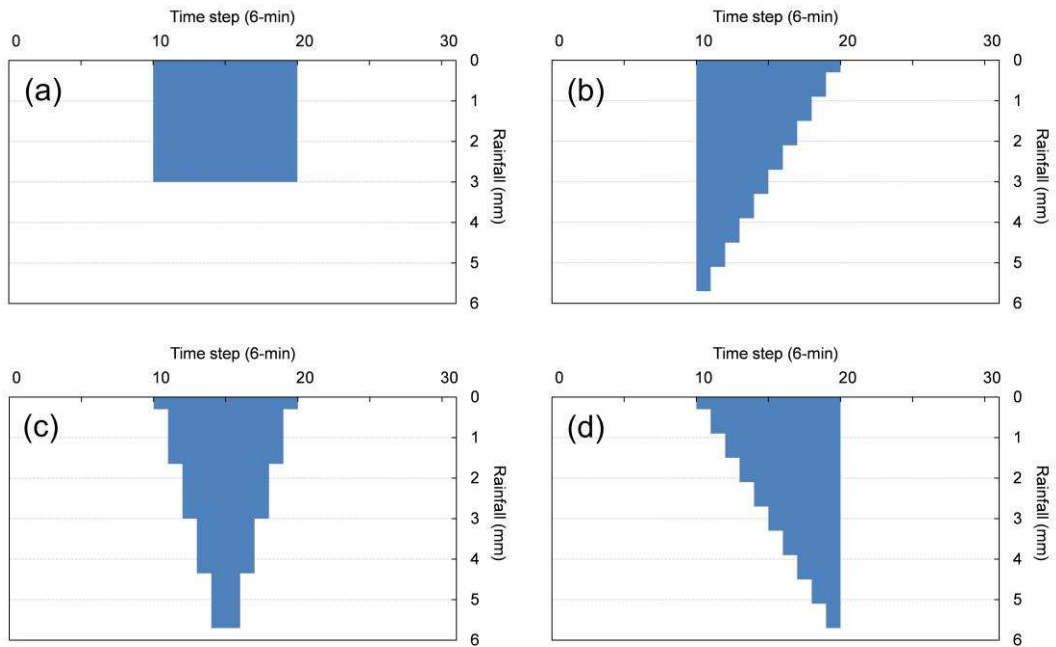
834

835 **Figures**



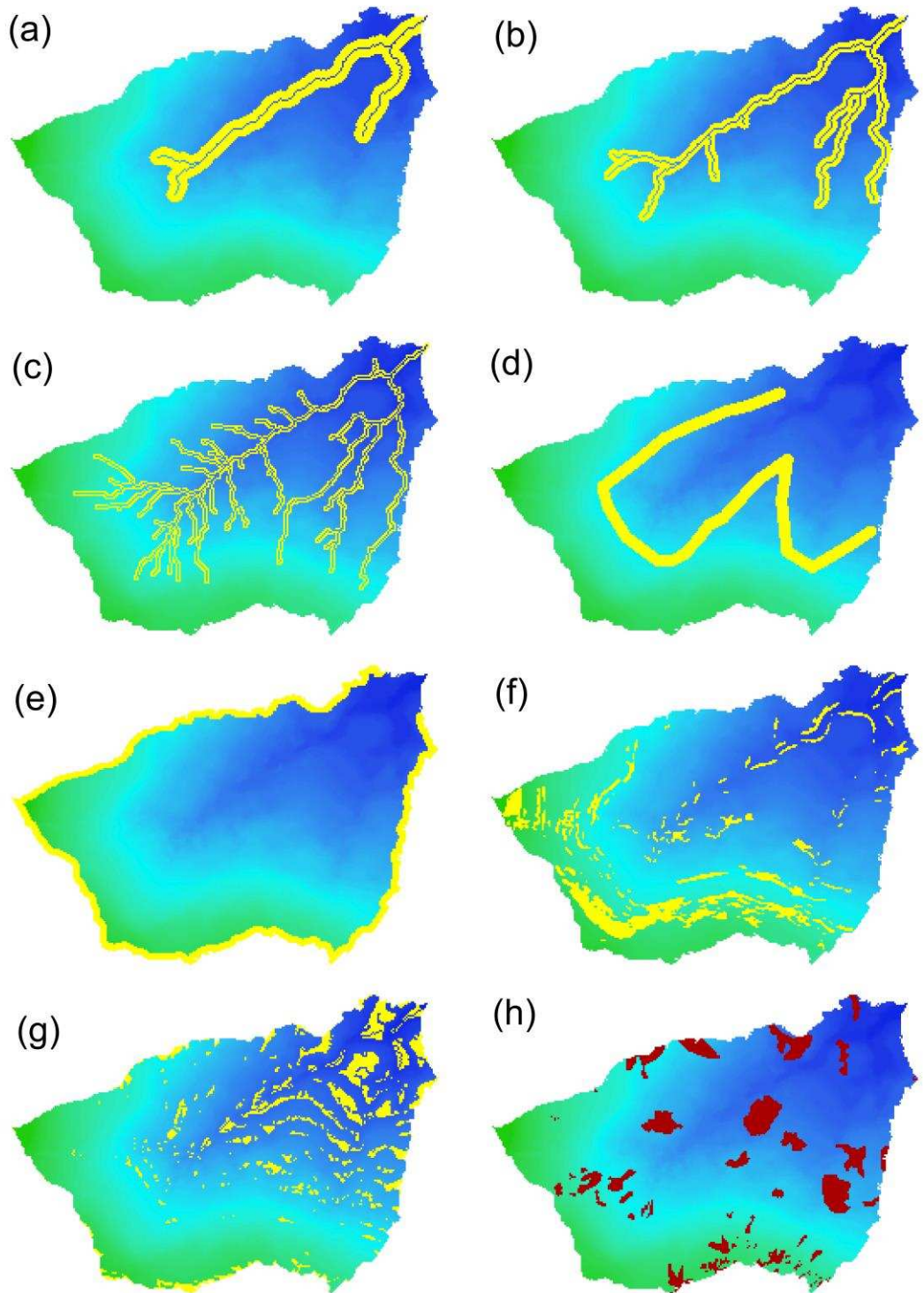
836

837 Figure 1. Location and map of the Trout Beck catchment.



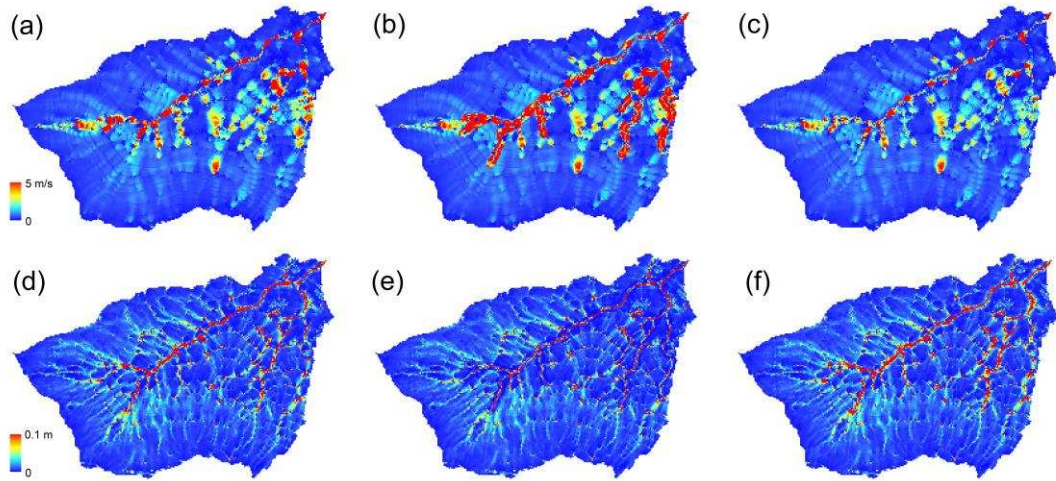
838

839 Figure 2. Precipitation patterns of the 30 mm rainfall for scenario modelling  
840 runs; (a) uniform, (b) early peak, (c) middle peak, and (d) late peak.



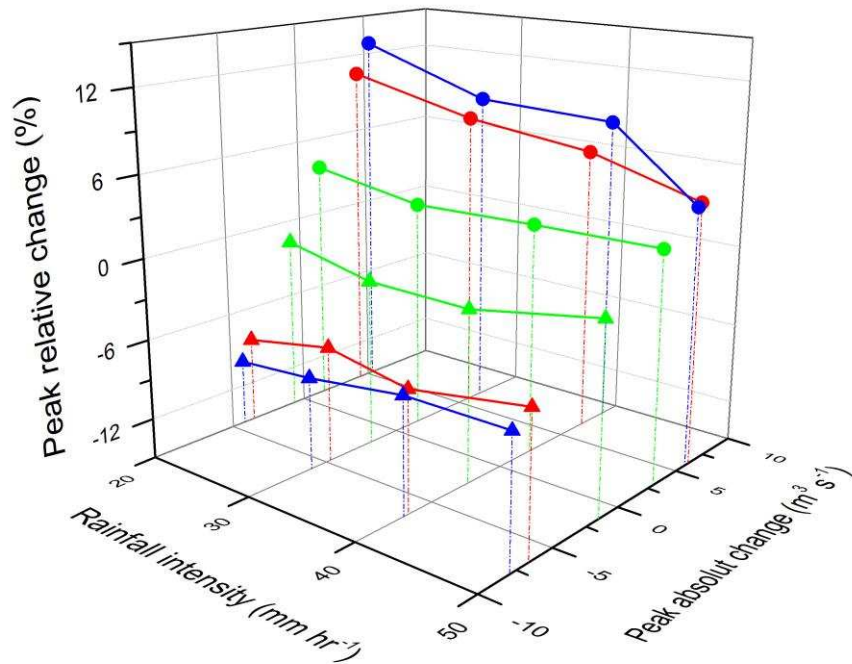
841

842 Figure 3. The slope position scenarios, the riparian zone scenarios, the  
843 steep-gentle slope scenarios and the real bare peat scenario in Trout  
844 Beck; (a) riparian strip (3000-cell cumulative area draining to the  
845 channel network), (b) riparian strip (1000-cell cumulative area  
846 draining to the channel network), (c) riparian strip (250-cell cumulative area  
847 draining to the channel network), (d) mid-hillslope strip, (e) headwater  
848 strip, (f) steepest slope area, (g) gentlest slope area, (h) bare peat  
849 distribution.



850

851 Figure 4. Distribution maps of overland flow velocity (a, b, and c) and depth  
852 (d, e, and f) for the baseline scenario, the 250-cell bare peat riparian  
853 strip scenario, and the 250-cell *Sphagnum* riparian strip scenario after  
854 30mm uniform rainfall (i.e. at time step 21).



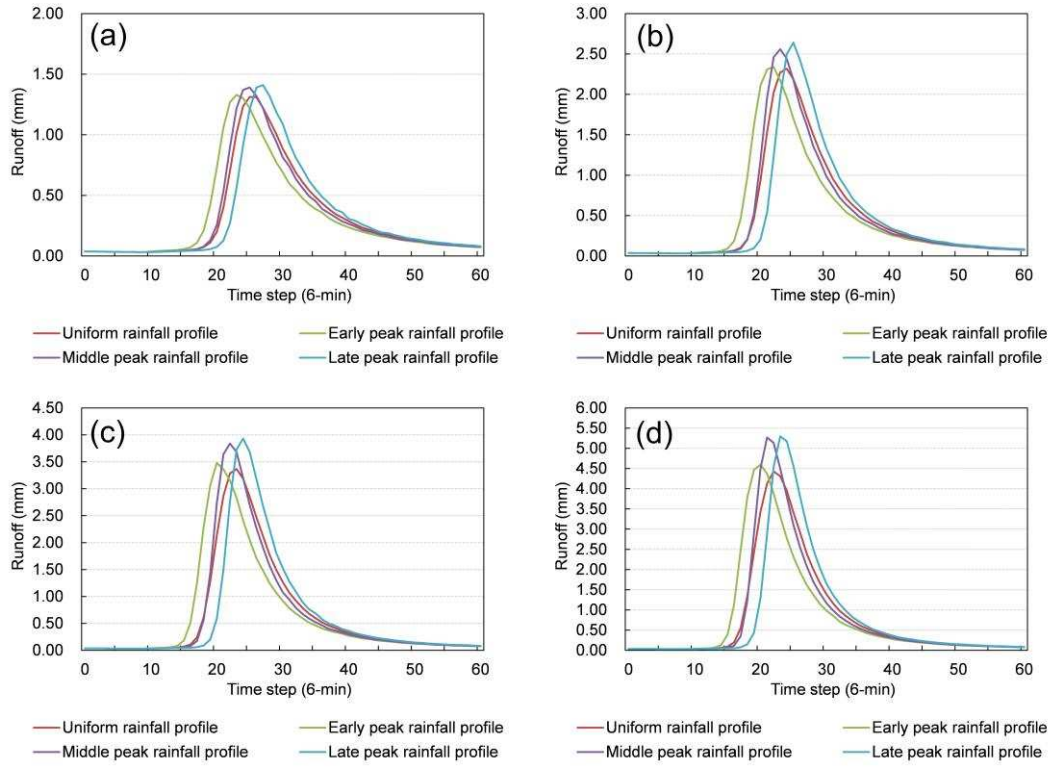
855

- Bare buffer strip (250 channel)
- Bare flattest slopes
- Headwater bare strip
- Sph. buffer strip (250 channel)
- Sph. flattest slopes
- Headwater Sph. strip

856  
857

Figure 5. Scenario comparison of the impacts on peak flow under different rainfall intensities.





858

859

860

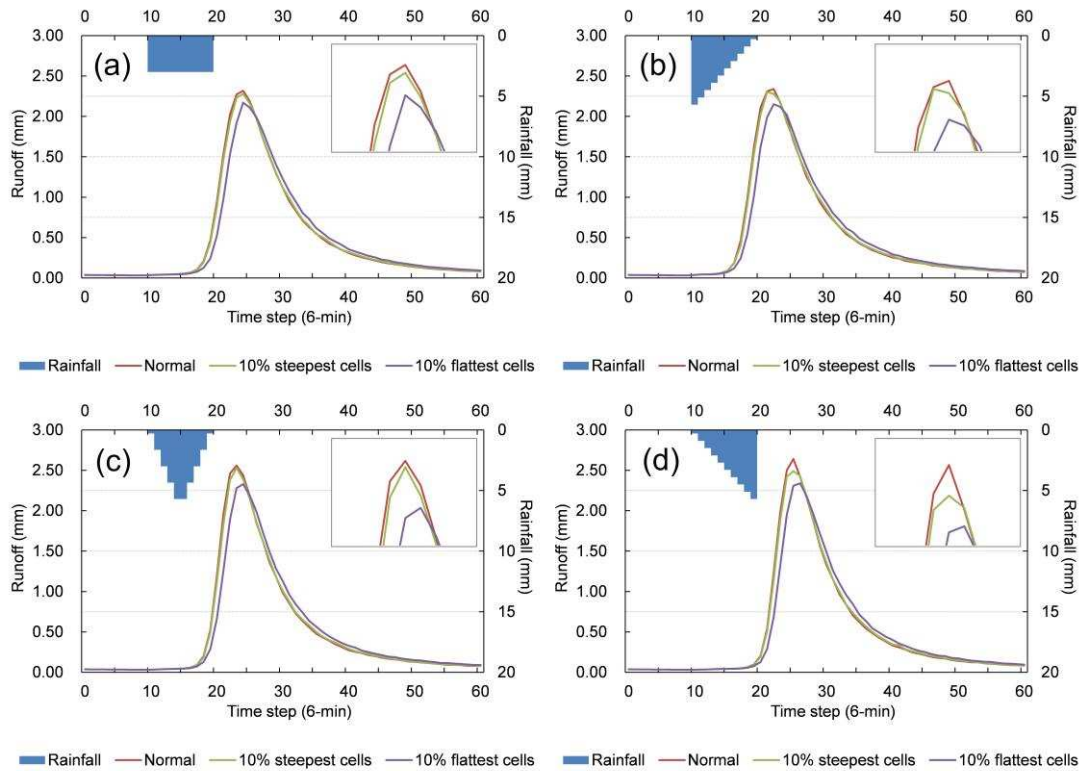
861

862

863

864

Figure 6. Hydrographs for the baseline land-cover scenario under different precipitation profiles with varying total rainfall depths; (a) 20 mm, (b) 30 mm, (c) 40 mm, and (d) 50 mm.



865

866

867

868

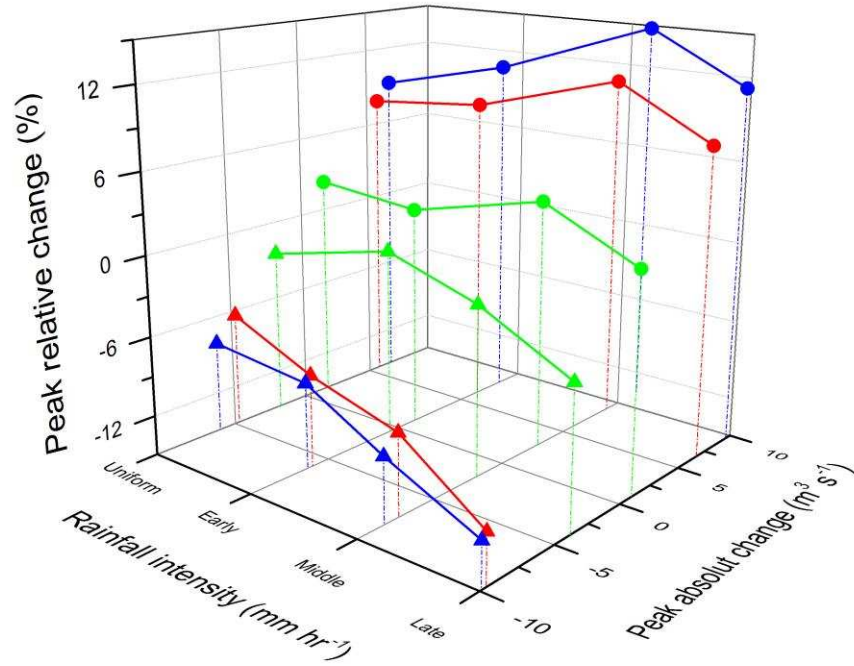
869

870

871

872

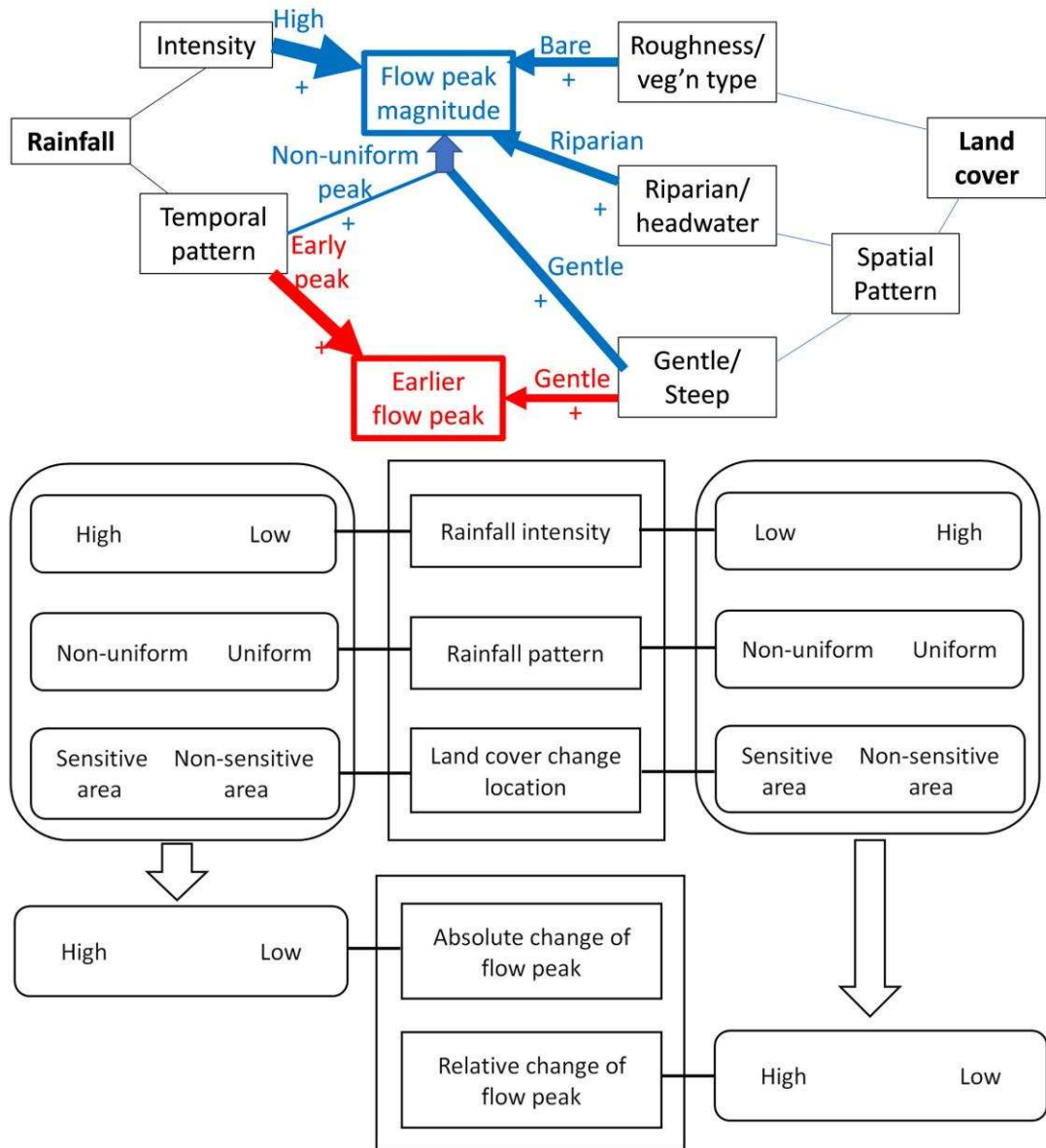
Figure 7. Hydrographs of the slope scenarios (*Sphagnum* on the 10% steepest areas and on the 10% flattest areas of the catchment) under 30 mm rainfall events with different precipitation profiles; (a) uniform rainfall profile, (b) early peak rainfall profile, (c) middle peak rainfall profile, and (d) late rainfall peak profile. Note: the runoff scale of the nested plot focusing on the hydrograph peaks on the upper right corner is 0.5 mm.



- Bare buffer strip (250 channel)
- Bare flattest slopes
- Headwater bare strip
- ▲ Sph. buffer strip (250 channel)
- ▲ Sph. flattest slopes
- ▲ Headwater Sph. strip

873

874 Figure 8. Scenario comparison of the impacts on peak flow under the 30 mm  
875 rainfall events with different rainfall patterns.



876

877 Figure 9. Conceptual diagrams showing the interaction effects of rainfall and  
 878 land-cover characteristics on peak river flow.

879